High-temperature high-sensitivity AlN-on-SOI Lamb wave resonant strain sensor

Cite as: AIP Advances **8**, 065315 (2018); https://doi.org/10.1063/1.5037721
Submitted: 26 April 2018 • Accepted: 07 June 2018 • Published Online: 18 June 2018

Shaoxu Dou, Mengke Qi, Cong Chen, et al.

High-temperature high-sensitivity AlN-on-SOI Lamb wave resonant strain sensor

Shaoxu Dou,[1] Mengke Qi,[1] Cong Chen,[1] Hong Zhou,[1] Yong Wang,[2] Zhengguo Shang,[1] Jing Yang,[3] Dengpan Wang,[3] and Xiaojing Mu[1,a]
[1]*Key Laboratory of Optoelectronic Technology & Systems, Ministry of Education and International R & D Center of Micro-Nano Systems and New Materials Technology, Chongqing University, Chongqing 400044, China*
[2]*IHP - Innovations for High Performance Microelectronics, Leibniz Association, Frankfurt (Oder) 15236, Germany*
[3]*Chongqing Acoustic-Optic-Electric Co. Ltd., China Electronic Technology Group Corp., Chongqing 400060, China*

(Received 26 April 2018; accepted 7 June 2018; published online 18 June 2018)

A piezoelectric AlN-on-SOI structured MEMS Lamb wave resonator (LWR) is presented for high-temperature strain measurement. The LWR has a composite membrane of a 1 μm thick AlN film and a 30 μm thick device silicon layer. The excited acoustic waves include Rayleigh wave and Lamb waves. A tensile strain sensor has been prepared with one LWR mounted on a uniaxial tensile plate, and its temperature characteristics from 15.4°C to 250°C and tensile strain behaviors from 0 με to 400 με of Rayleigh wave and S_4 mode Lamb wave were tested. The temperature test verifies the adaptability of the tensile strain sensor to temperature up to 250°C, and S_4 mode Lamb wave and Rayleigh wave represent almost the same temperature characteristics. The strain test demonstrates that S_4 mode Lamb wave shows much higher strain sensitivity (-0.48 ppm/με) than Rayleigh wave (0.05 ppm/με) and confirms its advantage of strain sensitivity. Finally, for this one-LWR strain sensor, a method of beat frequency between S_4 mode Lamb wave and Rayleigh wave is proposed for temperature compensation and high-sensitivity strain readout. https://doi.org/10.1063/1.5037721

Strain sensors operating at temperatures above several hundred degrees Celsius are demanded for industrial process monitoring and control, steel and refractory material manufacturing, in power plant environments, aerospace and defense.[1–4] The current high-temperature strain sensors include resistance strain gauge,[5] Fiber Bragg Grating (FBG) optical strain sensor[6] and surface acoustic wave (SAW) strain sensor.[7] SAW strain sensor has attracted considerable attention due to its properties of being passive and wireless, low cost and good reproducibility.

Most of SAW strain sensors can only work below 150°C due to the limit of the conventional piezoelectric materials such as quartz, lithium niobate (LN) and zinc oxide (ZnO).[8–11] Aluminum nitride (AlN) is a promising high-temperature piezoelectric material with a Curie temperature close to 1200°C.[12,13] AlN film can also be grown on various substrates such as Si, SiC, sapphire and diamond, and the growth processes are compatible with the micro-fabrication process.[14–17] SAW sensors based on AlN film with working temperatures up to 500°C have been reported[18,19] and verified the feasibility for high-temperature strain measurement.

However, there have been no reports of AlN-based Lamb wave strain sensor. In our previous study on AlN-based Lamb wave pressure sensor, the high order mode Lamb wave demonstrated a pressure sensitivity 1.7 times higher than the surface acoustic wave (specifically, the Rayleigh wave).[20] Mohabuth et al. also reported that higher-order Lamb waves show a higher sensitivity to

[a]Corresponding author: mxjacj@cqu.edu.cn

applied stresses.[21] Thus the development and study of a AlN-on-SOI structured Lamb wave strain sensor is necessary.

In this letter, we design and fabricate a piezoelectric AlN-on-SOI structured MEMS Lamb wave resonator (LWR) for high-temperature strain measurement. A tensile strain sensor has been prepared with one LWR mounted on a uniaxial tensile plate, and its temperature characteristics from 15.4°C to 250°C and tensile strain behaviors from 0 με to 400 με of Rayleigh wave and S_4 mode Lamb wave have been tested. The results show that the tensile strain sensor has the temperature adaptability up to 250°C, and that S_4 mode Lamb wave shows much higher strain sensitivity than Rayleigh wave which confirms its advantage of strain sensitivity. Finally, a beat frequency method for temperature compensation and high-sensitivity strain readout is proposed for this one-LWR strain sensor.

Figure 1 shows the 3D schematic illustration and scanning electron micrograph (SEM) image of the AlN-on-SOI structured Lamb wave resonator (LWR). The electrode width and spacing of the Interdigitated Transducer (IDT) and reflectors are designed to be 2.6 μm. The aperture and number of the IDT electrode are 1280 μm and 128 pairs respectively.

The LWR fabrication process is compatible with the CMOS process. A 4 in. SOI (100) wafer with a 30 μm thick device Si layer, a 1 μm thick buried oxide (BOX) layer and a 400 μm thick handle Si layer was employed. A 100 nm thick SiO_2 film was deposited on the device Si layer by plasma enhanced chemical vapor deposition (PECVD). A 200 nm thick Mo film was deposited on the SiO_2 film as a bottom electrode layer. A 1 μm thick AlN (002) film was deposited on the Mo film by magnetron sputtering process. A 150 nm thick Mo film was deposited on the AlN film and patterned by dry etching to form the IDT and reflectors. A 300 nm thick SiO_2 film was deposited as a passivation layer on the IDT structure by PECVD process. After the aforementioned front side process, a 2 μm thick SiO_2 film was deposited on the backside of the SOI wafer and patterned for the release process. The device Si layer right below the IDT's center was released by deep reactive ion etching (DRIE) process on the backside of the handle Si wafer, and a AlN/Si composite membrane with a diameter of 1 mm was formed. The SiO_2 passivation layer above the IDT structure was patterned by vapor hydrogen fluoride (HF) for contact open. Finally, a 200 nm thick Au film was deposited on the SiO_2 passivation layer and patterned for wire-bonding. After the micro-fabrication process, the LWRs were diced from the SOI wafer.

As shown in Figure 2, a uniaxial tensile strain sensor was prepared with a LWR and a printed circuit board (PCB) signal port adhered onto a tensile plate specimen by high-temperature

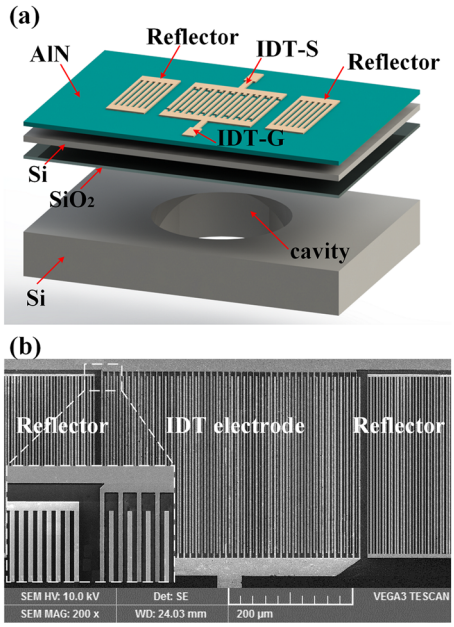

FIG. 1. (a) 3D illustration of the AlN-on-SOI LWR; (b) SEM of the IDT electrodes and reflectors.

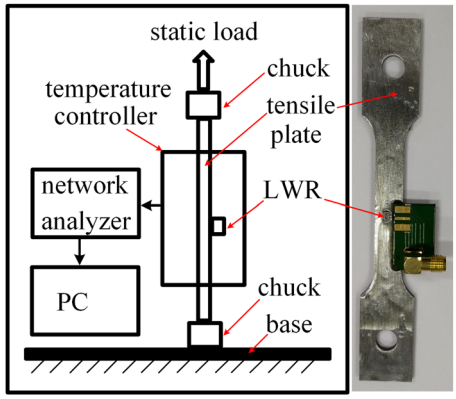

FIG. 2. Illustration of the strain measurement and the photo of the strain sensor.

epoxy glue. The LWR was placed with its acoustic wave propagating direction parallel to the tensile axis. The tensile plate specimen was made of mild steel (ISO630 E235B) with a Young's modulus of 203.2 GPa, a Poisson's ratio of 0.28, a cross-section area of 2.5 mm×10 mm and a length of 50 mm. Wire-bonding process was used to connect the LWR to the PCB signal port, and a SMA connector was soldered onto the PCB signal port to connect with an Agilent E5071B network analyzer. The tensile strain sensor was then mounted on a high-temperature tensile tester for temperature test and strain test (Figure 2). The chamber temperature and tensile strain applied to the tensile strain sensor were controlled by using three heating modules and one strain module.

The S_{11} parameters of the strain sensor at room temperature (15.4°C) and under no-load were measured, and Rayleigh wave and the most obvious Lamb wave were determined at 435.2 MHZ and 896.1 MHz respectively. This Lamb wave is supposed to be S_4 mode Lamb wave, according to the simulated acoustic wave mode shapes in the AlN/Si composite membrane[15] (figure 3) by using the software COMSOL Multiphysics. The COMSOL simulation setup and material properties used can be referred in the prior arts.[22,23]

To determine the temperature behaviors of the strain sensor, the S_{11} parameters of Rayleigh wave and S_4 mode Lamb wave at room temperature (15.4°C), 100°C, 150°C, 200°C and 250°C and under no-load were measured respectively. Note that 250°C was chose as the maximum temperature because of the temperature limit of the PCB signal port, the SMA connector and the RF signal wire which were also subjected to the same high temperatures as the LWR, and that the measurement was carried out after 30 min holding time at each temperature point and that the minimum values of the S_{11} parameters were selected as the resonance frequencies. The relationship between the resonance frequency of Rayleigh wave and the temperature is shown in

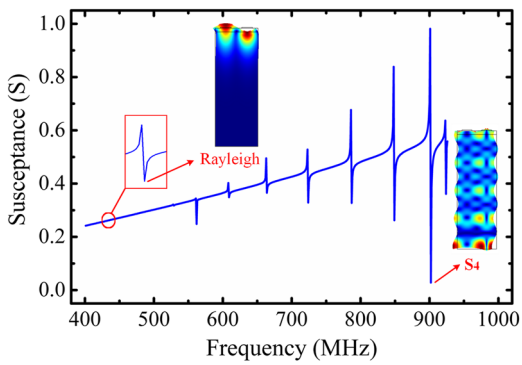

FIG. 3. Simulated frequency spectrum of the LWR with the insets showing the resonance mode shapes.

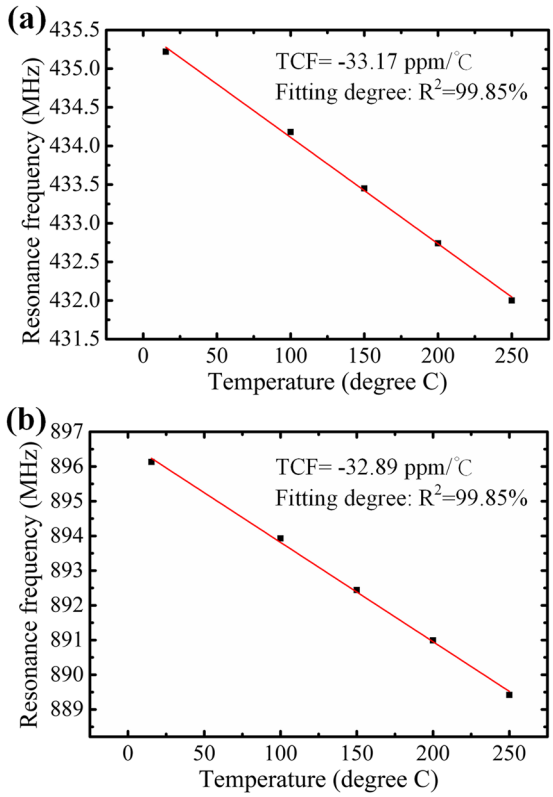

FIG. 4. Measured temperature behavior for (a) Rayleigh wave and (b) S_4 mode Lamb wave.

figure 4(a). With the temperature increasing, the resonance frequency decreases linearly. The approximated first-order temperature coefficient of frequency (TCF) is extracted to be -33.17 ppm/°C (-14.4 KHz/°C), which is a comparable result with what has been reported in literature.[20] Meanwhile, S_4 mode Lamb wave shows almost the same temperature characteristic with Rayleigh wave due to the same material stack (see Figure 4(b)). Specifically, the ratios of the resonance frequency of S4 mode Lamb wave to those of Rayleigh wave at any temperature and are approximately constants of 2.0589.

To characterize the tensile strain responses, the S_{11} parameters of Rayleigh wave and S_4 mode Lamb wave at room temperature (15.4°C) and under the tensile loading of 0 με, 100 με, 200 με, 300 με and 400 με were measured respectively. Note that the measurement was carried out after 5 min holding time at each strain level and that the minimum values of the S_{11} parameters were selected as the resonance frequencies. The relationship between the resonance frequencies of Rayleigh wave and S_4 mode Lamb wave and the tensile strain are demonstrated in figure 5. Rayleigh wave has a positive strain coefficient of frequency (SCF) of +0.05 ppm/με (+0.027 kHz/με) whereas S_4 mode Lamb wave shows a negative SCF of -0.48 ppm/με (-0.431 kHz/με). Obviously, S_4 mode Lamb wave gives an 8.6 times enhancement in strain sensitivity over Rayleigh wave. This sensitivity value is also higher than that of SAW strain sensor in literature[14] and verifies the sensitivity advantage of S_4 mode Lamb wave. This may be due to the fact that S_4 mode Lamb wave is near the cut-off frequency and has much higher phase velocity sensitivity to uniaxial stress.[21]

As discussed above, we can achieve a high strain sensitivity with S_4 mode Lamb wave. However, when the strain sensor operates in the range from room temperature to 250°C, the temperature-induced frequency shift is significant and thus the temperature compensation for the strain readout is necessary. Assuming that the temperature change Δt and the tensile strain change $\Delta\varepsilon$ influence the resonance frequencies independently, the resonance frequencies of S_4 mode Lamb wave and Rayleigh wave can be expressed as

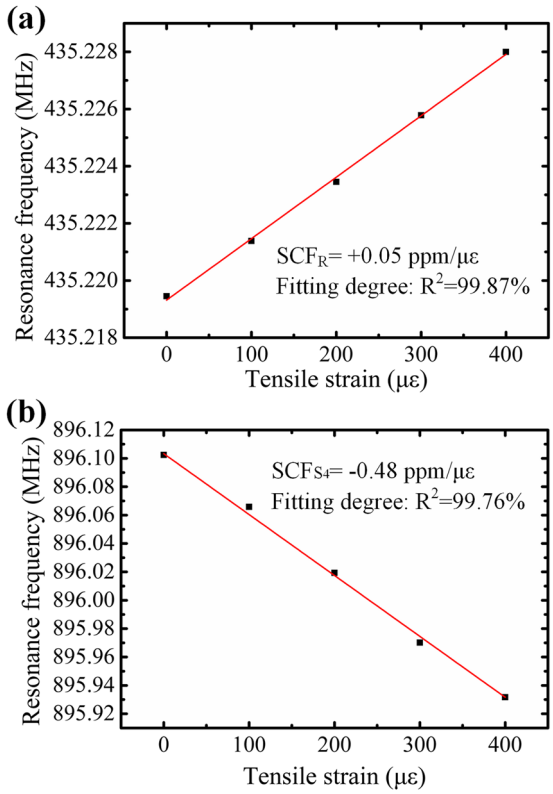

FIG. 5. Measured strain behavior for (a) Rayleigh wave and (b) S_4 mode Lamb wave.

$$f_S(t,\varepsilon) = f_S(t_0,\varepsilon_0) + f_S(\Delta t) + f_S(\Delta\varepsilon) \tag{1}$$

$$f_R(t,\varepsilon) = f_R(t_0,\varepsilon_0) + f_R(\Delta t) + f_R(\Delta\varepsilon) \tag{2}$$

where $f_S(t,\varepsilon)$ and $f_R(t,\varepsilon)$ are the resonance frequencies of S_4 mode Lamb wave and Rayleigh wave respectively at the temperature t and under the tensile strain ε; $f_S(t_0,\varepsilon_0)$ and $f_R(t_0,\varepsilon_0)$ are the resonance frequencies of S_4 mode Lamb wave and Rayleigh wave respectively at the reference temperature t_0=15.4°C and under the initial tensile strain ε_0=0; $f_S(\Delta t)$ and $f_R(\Delta t)$ are the resonance frequency shifts of S_4 mode Lamb wave and Rayleigh wave induced by the temperature change $\Delta t = t - t_0$ respectively; and $f_S(\Delta\varepsilon)$ and $f_R(\Delta\varepsilon)$ are the resonance frequency shifts of S_4 mode Lamb wave and Rayleigh wave induced by the tensile strain change $\Delta\varepsilon = \varepsilon - \varepsilon_0$ respectively.

According to figure 4, the relationship between S_4 mode Lamb wave and Rayleigh wave can be expressed as

$$\frac{f_S(t_0,\varepsilon_0)}{f_R(t_0,\varepsilon_0)} = \frac{f_S(\Delta t)}{f_R(\Delta t)} \approx 2.0589 \tag{3}$$

According to figure 5, $f_S(\Delta\varepsilon)$ and $f_R(\Delta\varepsilon)$ can be expressed as

$$f_S(\Delta\varepsilon) = f_S(t_0,\varepsilon_0) \cdot SCF_S \cdot \Delta\varepsilon \tag{4}$$

$$f_R(\Delta\varepsilon) = f_R(t_0,\varepsilon_0) \cdot SCF_R \cdot \Delta\varepsilon \tag{5}$$

where SCF_S and SCF_R are the strain coefficients of frequencies of S_4 mode Lamb wave and Rayleigh wave respectively.

The beat frequency Δf is defined as

$$\Delta f = f_S(t,\varepsilon) - 2.0589 \cdot f_R(t,\varepsilon) \tag{6}$$

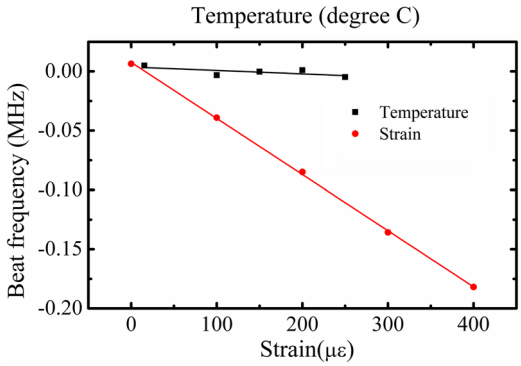

FIG. 6. Beat frequency for temperature and strain predicted from the temperature and strain measurement.

Substituting equations (1)–(5) into equation (6), Δf can be rewritten as

$$\Delta f = f_S(t_0, \varepsilon_0) \cdot (SCF_S - SCF_R) \cdot \Delta\varepsilon \tag{7}$$

Comparing equation (6) with (7), it can be found that Δf is a linear function of strain change $\Delta\varepsilon$ but is independent of temperature change Δt. Thus we can achieve temperature compensation as well as strain readout. Moreover, as SCF_S and SCF_R are opposite in sign in equation (7), further enhancement in strain sensitivity is obtained, that is (-0.48-0.05) = -0.53 ppm/με. As an example, figure 6 shows the predicted Δf versus temperature and strain from the measured results. The Δf predicted from figure 4 remains approximately constant, implying that it is relatively insensitive to the temperature change; whereas the Δf predicted from figure 5 exhibits a slope of -0.46 kHz/με, confirming its high sensitivity to the tensile strain.

In summary, we demonstrate a piezoelectric AlN-on-SOI structured Lamb wave resonator for high-temperature strain measurement. A tensile strain sensor has been prepared with this LWR and the temperature characteristics and strain behaviors of Rayleigh wave and S_4 mode Lamb wave have been tested. The temperature test verifies the adaptability of this sensor to temperature up to 250°C, and the strain test confirms the high sensitivity of S_4 mode Lamb wave. Finally, a beat frequency method is proposed to realize temperature-compensated high-sensitivity strain readout with this one-LWR sensor.

This work was supported by National Key Research and Development Program of China (Grant No. 2016YFB0402702), National Natural Science Foundation of China (Grant No. 51605060), Fundamental Research Funds for the Central Universities (No. 106112016CDJZR125504), Ministry of Education of the People's Republic of China, Key technology innovation projects of key industries in Chongqing under Grant cstc2016zdcy-ztzx0034 and the "thousands talents" program for the pioneer researcher and his innovation team, China.

[1] S. Basu and A. K. Debnath, *Power Plant Instrumentation and Control Handbook* (1st ed.) (Academic Press, 2014).
[2] A. K. Elshennawy and G. S. Weheba, *Manufacturing Processes and Materials* (5th ed.) (SME, Dearborn, MI, 2015).
[3] W. C. Wilson, M. D. Rogge, B. H. Fisher, D. C. Malocha, and G. M. Atkinson, IEEE Sens. J. **12**, 1993 (2012).
[4] S. J. Mihailov, Sensors **12**, 1898 (2012).
[5] HITEC Products INC., Strain Gages for Static Strain Measurements (2017). (Online). Available: http://www.hitecprod.com/pages/static.html [accessed Dec. 2015].
[6] J. Huang, Z. Zhou, D. Zhang, and Q. Wei, Adv. Mech. Eng. **5**, 1 (2013).
[7] A. Maskay and M. P. D. Cunha, Sensor. Actuat. A-Phys. **259**, 34 (2017).
[8] S. Zhang and F. Yu, J. Am. Ceram. Soc. **10**, 3153 (2011).
[9] H. Oh, K. Lee, K. Eun, S. H. Choa, and S. S. Yang, J. Micromech. Microeng. **22**, 025002 (2012).
[10] C. Fu, K. J. Lee, K. Eun, S. H. Choa, K. Lee, and S. S. Yang, J. Appl. Phys. **120**, 024501 (2016).
[11] R. Stoney, D. Geraghty, and G. E. O'Donnell, IEEE Sens. J. **14**, 722 (2014).
[12] Y. J. Lai, W. C. Li, C. M. Lin, V. V. Felmetsger, and A. P. Pisano, in Proceedings of Transducers 2013 (2013), pp. 2268–2271.
[13] R. C. Turner, P. A. Fuierer, R. E. Newnham, and T. R. Shrout, Appl. Acoustic. **41**, 299 (1994).
[14] Z. Bao, M. Hara, and H. Kuwano, in Proceedings of Transducers 2015 (2015), pp. 1239–1242.
[15] C. M. Lin, Y. Y. Chen, V. V. Yantchev, D. G. Senesky, and A. P. Pisano, Adv. Mater. **24**, 2722 (2012).
[16] T. Aubert, J. Bardong, O. Legrani, O. Elmazria, M. B. Assouar, G. Bruckner, and A. Talbi, J. Appl. Phys. **114**, 358 (2013).
[17] T. Wang, X. Mu, A. B. Randles, Y. Gu, and C. Lee, Appl. Phys. Lett. **107**, 123501 (2015).

[18] S. Chen and Z. You, Sensors **16**, 1205 (2016).
[19] C. Li, X. Zhao, B. Peng, L. Shu, and Y. Rong, Rare Met. **35**, 408 (2016).
[20] X. Mu, P. Kropelnicki, Y. Wang, A. B. Randles, K. T. C. Chai, H. Cai, and Y. Gu, Appl. Phys. Lett. **105**, 113507 (2014).
[21] M. Mohabuth, A. Kotousov, and C. Ng, Int. J. Non-Linear Mech. **86**, 104 (2016).
[22] D. K. Pandey and R. R. Yadav, Appl. Acoust. **70**, 412–415 (2009).
[23] J. Bjurstrom, G. Wingqvist, V. Yantchev, and I. Katardjiev, J. Micromech. Microeng. **17**, 651 (2007).